

Appendix J

Thermal issues related to ExoMars EDLS performance

Emilie Boulier Grégory Pinaud Patrick Bugnon
(Airbus Defence & Space, France)

Abstract

During its planetary entry, EXoMars heatshield encounters specific hypersonic environments, in terms of aerothermochemistry, radiation, particule flows... and therefore requests a specific effort, in relation to aerodynamic characterisation and quantification of thermal / thermomechanical loads, as well as demonstration of thermostructural integrity and thermal efficiency.

Airbus Defense & Space is a major contributor to both issues.

The present communication aims at emphasizing two important axes of progress :

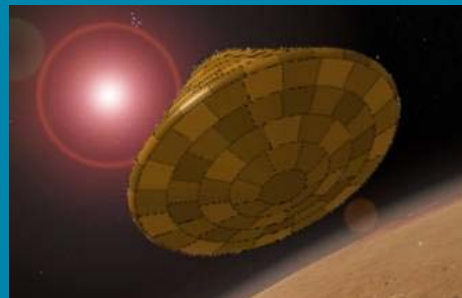
- Performance of the vehicle & application thanks to TPS optimisation
 - Updated material data sets could be derived from dedicated tests
 - Material data sets were integrated to thermophysical modelisations
 - Improved thermophysical modelisations allowed TPS thickness reduction
- Quality of planned postflight analysis, thanks to advanced modelisation including parametric and statistic analyses, inverse methodologies, cosimulation.

28th European Space Thermal Analysis Workshop
 14-15 October 2014 - ESA/ESTEC

Thermal issues related to ExoMars EDLS Performance

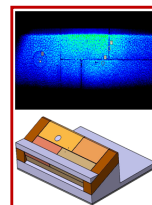
E. Boulier, G. Pinaud, P. Bugnon

AIRBUS Defence & Space – Thermal & Thermo-mechanical Engineering
 Aquitaine Site



SUMMARY

INTRODUCTION	EXOMARS MISSION
OBJECTIVE	EXOMARS FRONTSHIELD OPTIMIZATION
LOGIC	DEDICATED THERMAL TEST & MODELLING
TEST	MODELLING SIMOUN PLASMA FACILITY
MATERIAL	MODELLING NORCOAT-LIEGE SPECIMEN
FUTURE	POST-FLIGHT RECONSTRUCTION



Date/Time

2

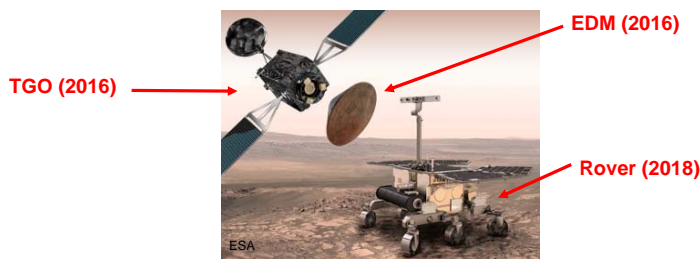
EXOMARS MISSION

14/03/2013 : ESA & ROSCOSMOS sign a cooperation agreement

- 2016 mission under ESA leadership
 - Satellite TGO (Trace Gaz Orbiter)
 - Demonstrator EDM (Entry & Descent Demonstrator Module)
- 2018 mission under ROSCOSMOS leadership
 - Russian EDM, ESA Rover on board



Both missions involve russian launcher PROTON



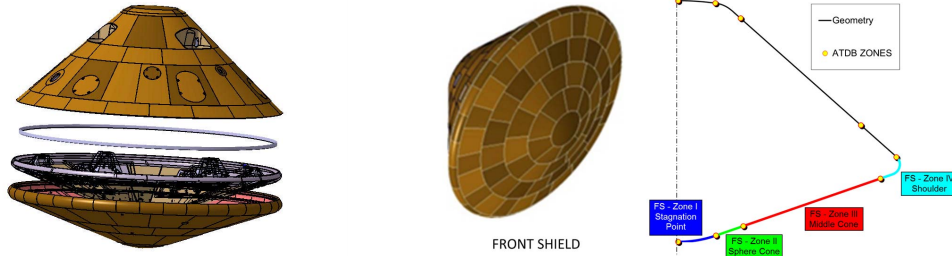
EXOMARS MISSION



- Hypervelocity entry
- Detached bow shock
- Dissociation and ionization
- Shock layer radiation
- Surface recombination
- Ablation/Pyrolysis boundary layer interaction
- Boundary layer transition
- Separation
- Shock layer viscous interaction
- Flow recombination



EXOMARS FRONTSHIELD OPTIMIZATION



Mars planetary entry includes environment specificities such as dust, CO₂ atmosphere, significant radiation.

Hypersonic kinetic energy → thermal energy (98%) → aerothermal flux (10%) → conduction inside heatshield (10%)

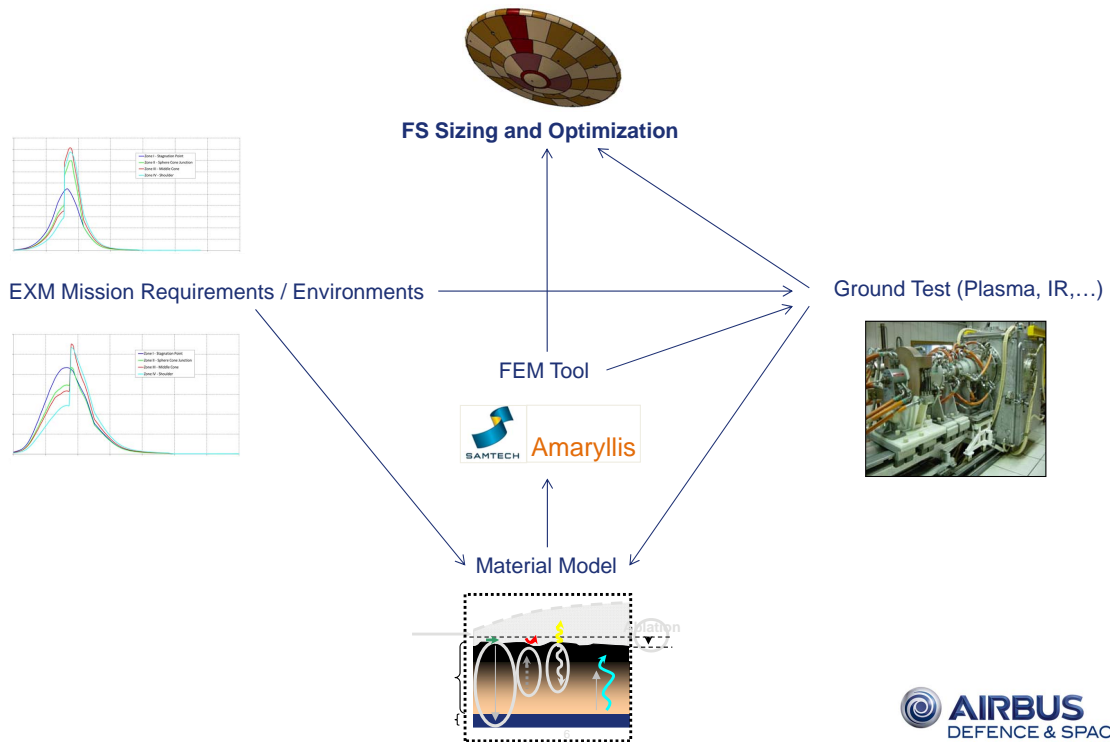
Peak load values during entry are 1,8 MW/m² for aerothermal flux, 7800 kg for integrated pressure on frontshield. Expected frontshield temperature variations are [-110°C;+1750°C] for TPS, [-110°C;+180°C] for structure.

Frontshield diameter and mass are 2,4 m and 80 kg (~ 40 kg structure, ~ 40 kg TPS).
 TPS consists of 90 tiles of outgassed NORCOAT-LIEGE fixed with ESP495, ACC Silicone glue.
 Instrumentation includes 7 thermoplugs (each embedding several thermocouples), 7 thermistors, 4 pressure sensors.

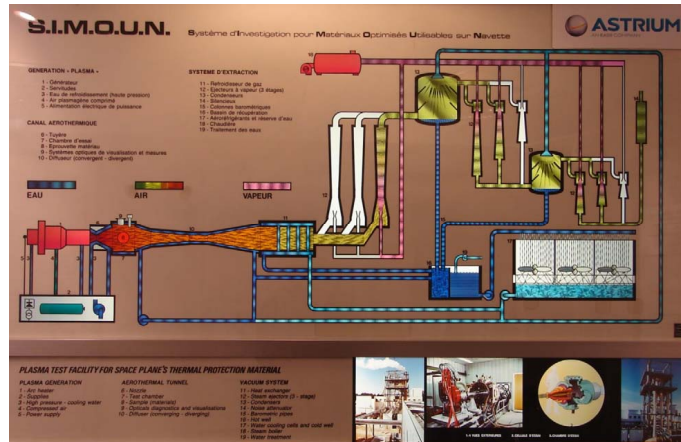
Presently discussed issue : determination of optimal NORCOAT-LIEGE thickness per zone.
 Application results in reducing TPS mass by ~ 8 kg (Payload mass ~ 10 kg)



EXM EDLS Logic



SIMOUN PLASMA FACILITY



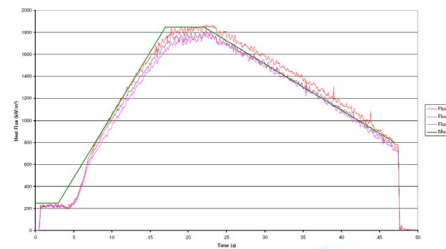
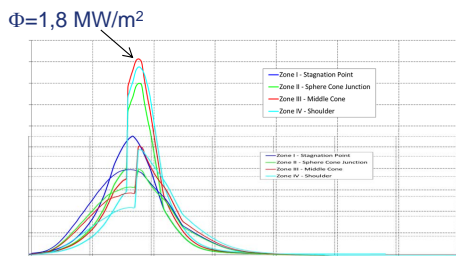
SIMOUN delivers a Mach 4, high enthalpy ($H_0/RT_0 \sim 100$), low pressure ($P_e \sim 0,1$ bar), air / CO_2 flow. Uniform conditions can be obtained on Flat Plate 30 cm wide samples, possibly using a wedge. A Stagnation Point configuration is as well available.

Date/Time

7

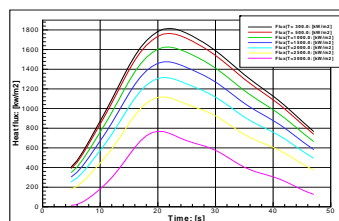
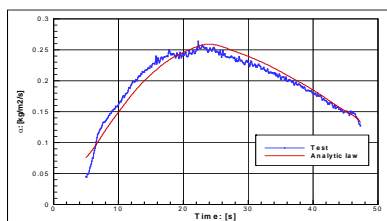


SIMOUN AEROTHERMAL MODEL



SIMOUN CO_2 test conditions deliver conservative, flight-representative aerothermal conditions on a Flat Plate sample, in terms of cold wall heat flux, shear stress, local pressure evolutions.

Calibration data (H_0/RT_0 , P_0 , T_{CW} , Φ_{CW} , P_e , Q), design data (nozzle expansion, wedge angle...), flow physical assumptions (frozen flow, heat flux formulas...) make possible an estimation of recovery enthalpy & convection coefficient. Estimated & experimental convection coefficients present similar evolutions, therefore a dependency of heat flux versus wall temperature can be derived from calibration data.



Date/T



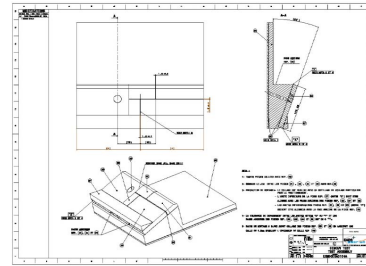
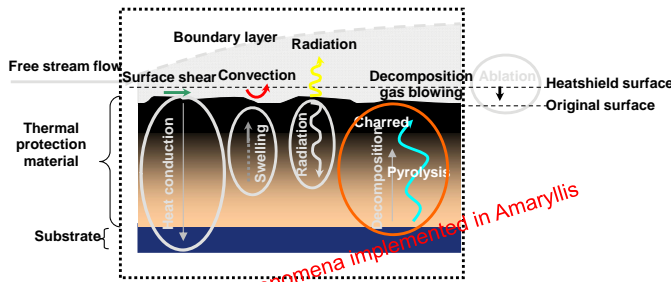
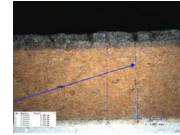
NORCOAT-LIEGE MATERIAL & SAMPLE

NORCOAT-LIEGE is a medium range insulator & ablator, in terms of admissible heat fluxes ($\Phi_{cw} < 2 \text{ MW/m}^2$).

NORCOAT-LIEGE composition mainly includes phenolic resin & cork particles.

NORCOAT-LIEGE behaviour under aerothermal loads classically includes :

- a high temperature increase of the material at the wall,
- a pyrolysis layer underneath the surface : the virgin material decomposes into gasses and a charred phase,
- a percolation of the pyrolysis gasses through the charred zone and a swelling of the pyrolysing material.



SIMOUN sample presents a wedge configuration for local pressure and heat flux flight-representativity purpose.

Sample includes joints, steps and gaps. Instrumentation includes thermoplugs (each embedding several thermocouples), pressure & ablation sensors.



MATERIAL THERMO-PHYSICAL MODEL

Conductivity & specific heat

Virgin properties are obtained from characterization ; charred properties are theoretical or extrapolated from virgin state.

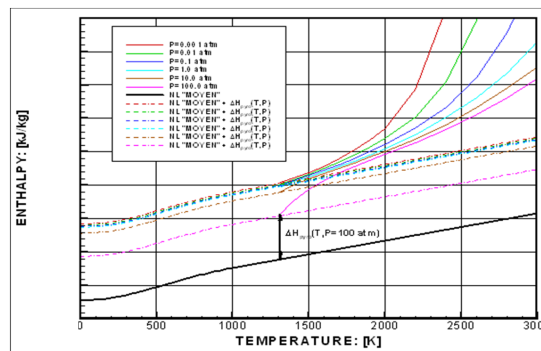
Pyrolysis

Mass loss kinetic is described as a multi-Arrhenius law from a series of TGA at several heating rates.

Reference enthalpies of virgin & charred material can be determined from molecular composition analysis.

Pyrolysis heat of material is evaluated on the basis of an "average" solid enthalpy and continuity considerations, from finite rate to equilibrium heterogeneous chemistry.

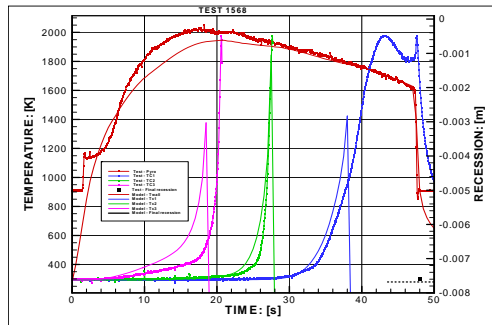
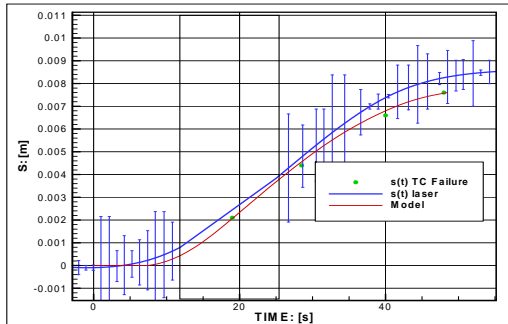
Enthalpy of pyrolysis gas (as a function of pressure & temperature) is derived from homogeneous chemical equilibrium conditions.



MATERIAL ABLATIVE MODEL

Experimental ablation evolution is obtained from laser recession sensor, location & failure time of thermocouples, post test micrographic cuts.

Model considers contributions of chemical and mechanical ablations, respectively depending on wall temperature and shear stress. Parameters are finally fitted from optimal matching of measured and calculated thermocouple temperature evolutions, under numerous aerothermal conditions.



$$\alpha(H_a - H_w) + \epsilon\sigma(T_r^4 - T_w^4) + \dot{m}_s[H_g] + \dot{m}_c[H_c] = -\lambda \frac{\partial T}{\partial x}$$

convection + radiation + pyrolysis + ablation = conduction



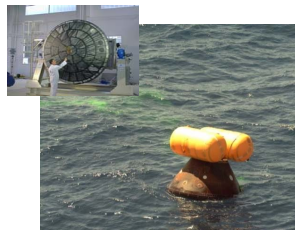
Date/Time

11

POST-FLIGHT RECONSTRUCTION



Huygens (1997-2005)



Atmospheric Reentry Demonstrator (1998)



French Deterrence Programs (since 1970s)

AIRBUS Defence & Space experience related to Post-flight analysis relies on a four decades continuous activity connected with miscellaneous Programs (ARD, military reentry vehicles & decoy systems).

Reconstruction of real flight conditions requires :

- multidisciplinary approaches,
- experience of inverse methods dedicated to loads rebuilding from structural responses,
- in-depth knowledge of “ground” justification models, in order to :
 - evaluate them with respect to flight restitution,
 - propose margin policies related to ground-flight extrapolation.



Date/Time

12

POST FLIGHT EDLS RECONSTRUCTION

TGO capabilities and EDLS sensors shall provide numerous parameters for post-flight reconstruction :

- (1) EDLS trajectory,
- (2) Atmospheric data,
- (3) Pressure evolutions on frontshield,
- (4) Temperature evolutions inside frontshield.

From (1), (2), (3), aerodynamic database shall be possibly updated and applied to the real trajectory.

Updated heat flux evolution shall be applied to « ground » model and shall result into thermoablative data (4') which shall be compared to flight data (4).

In-depth analysis of divergences shall allow identification of high priority modelling efforts to be achieved, for an improvement of performance on future missions.

Key tools are ready :

- Automatic parametric optimization of direct problem,
- Full numerical implementation of inverse problem coupled with optimization algorithm.

13



